

APPENDIX II

Part A

STRUCTURAL ANALYSIS OF THE  
BIG ROCK POINT NUCLEAR POWER PLANT  
SPENT FUEL POOL STRUCTURE

Amendment 2 - Dated January 1983

to

Big Rock Point Plant

Spent Fuel Rack Addition  
Consolidated Environmental  
Impact Evaluation  
Description and Safety Analysis

Consumers Power Company

ic1182-00-ia142

8301180400 830110  
PDR ADOCK 05000155  
P PDR

STRUCTURAL ANALYSIS OF THE  
BIG ROCK POINT NUCLEAR POWER PLANT  
SPENT FUEL POOL STRUCTURE

NUS-4247

January 4, 1983

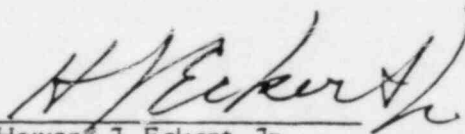
Prepared for:

CONSUMERS POWER COMPANY

Prepared by:

M.K. Prabhakara  
M.D. Liu  
T.K. Ghosh

Approved by:



Howard J. Eckert, Jr.  
Manager, Structural  
Engineering Department

NUS CORPORATION  
910 Clopper Road  
Gaithersburg, Maryland 20878

## TABLE OF CONTENTS

	<u>Page</u>
LIST OF TABLES	i
LIST OF FIGURES	i
1.0 INTRODUCTION	1-1
2.0 SUMMARY OF RESULTS	2-1
3.0 CONCLUSIONS	3-1
4.0 LOAD COMBINATIONS AND ACCEPTANCE CRITERIA	4-1
5.0 INPUT INFORMATION	5-1
6.0 MATHEMATICAL MODELING	6-1
6.1 <u>Finite Element Model</u>	6-1
6.2 <u>Support Conditions</u>	6-3
7.0 LOAD CONDITIONS	7-1
7.1 <u>Hydrostatic and Other Dead Loads</u>	7-2
7.2 <u>Thermal Loading</u>	7-3
8.0 SECTION STRENGTH CAPACITIES	8-1
8.1 <u>Moment Capacity</u>	8-1
8.2 <u>Shear Capacity</u>	8-3
8.3 <u>Required Development Length</u>	8-4
9.0 ANALYSIS METHODS	9-1
9.1 <u>Thermal Stress Analysis</u>	9-1
9.2 <u>Support Wall Analysis</u>	9-5
10.0 REFERENCES	10-1
FIGURES	

## LIST OF TABLES

<u>Table Number</u>	<u>Title</u>
1	Summary of Least Margins

## LIST OF FIGURES

<u>Figure Number</u>	<u>Title</u>
1	Finite Element Model
2	East-West Section through the Spent Fuel Pool
3	North-South Section through the Spent Fuel Pool
4	Plan at the Pool Floor Elevation
5	Plan Section below Elevation 598'-0"
6	Floor Support along the East and West Edges
7	Floor Support along the North and South Edges
8	Typical Temperature Gradients
9	Typical Variation of $T_{\text{mean}}$ and $\Delta T$ with Time
10	Typical Support Wall Model

## 1.0 INTRODUCTION

The purpose of the analysis reported herein is to determine the effect on the spent fuel pool structure of a postulated event in which the fuel pool wall temperature rises to 150°F. This rise in pool wall temperature causes a temperature gradient to develop through the thickness of the concrete slabs of the pool walls and the floor. Thermal moments and shear forces are developed in these structural elements due to the temperature gradient. The moments and shears for the thermal load are combined with the moments and shears due to the other mechanical loads. These combined moments and shears are checked against the moment and shear capacities at the various critical sections of the pool structure to determine the structural adequacy of the pool. Structural adequacy of the walls that support the pool is also checked.

A thermal analysis of the spent fuel pool structure was performed to determine the temperature distribution in the floor and walls. These temperatures are determined as a function of the time into the transient as well as through the thickness of the concrete slab based on a pool wall temperature of 150°F and ambient air temperature of 70°F.

The stress analysis of the spent fuel pool structure under the thermal and mechanical loading is performed by the finite element method. The ANSYS computer code was used for this purpose. The mechanical loads that are applied to the pool structure are dead weight and hydrostatic pressure. The dead load on the floor slab includes the weight of 31 ft. of water contained in the pool, the weight of the spent fuel racks (both the existing and the new), the weight of other equipment and the weight of the floor slab itself. The only dead load applied to the walls is the hydrostatic pressure due to water in the pool.

## 2.0 SUMMARY OF RESULTS

A summary of the least margins calculated for the pool floor, pool walls, and support walls is provided in Table 1. The shear and moment margins represent the ratios of the shear and moment capacities to the calculated values of shear and moment. The development length and splice length margins represent the ratios of the actual lengths to the required lengths. A margin greater than or equal to one therefore indicates acceptability.

For the pool floor and walls, all average shear, local shear, development length, and splice length margins are greater than one, as is the moment margin for the pool floor. Only at two locations in the south pool wall is the moment margin less than one. These locations are in a region of high internal restraint (i.e., at wall-to-wall) and in a region of discontinuity (i.e., at a transition in the thickness of the wall). Being that the area in which the capacity is exceeded is local, this condition is of little concern. The load that would have been carried in this area is distributed to the surrounding areas which are more than adequate to carry the load.

The support walls have margins greater than one with respect to all applicable parameters; namely shear, moment, and development length.

TABLE I SUMMARY OF LEAST MARGINS

	<u>Pool Floor</u>	<u>Pool Walls</u>	<u>Support Walls</u>
Shear, Average	2.10	1.42	1.63
Shear, Local	2.15	2.53	NA
Moment	1.57	0.23	1.51
Development Length (1)	1.18	1.25	1.87
Splice Length (2)	NA	1.06	NA

(1) see page 8-4.

(2) see page 8-5.

### 3.0 CONCLUSIONS

Based on the results presented in the previous section, it is concluded that the pool floor, pool walls, and support walls are adequate to withstand the postulated event in which the temperature of the pool wall rises to, and remains at, 150°F.



#### 4.0 LOAD COMBINATIONS AND ACCEPTANCE CRITERIA

The forces (or moments) for the various loading conditions are identified as follows:

D = Dead Load

Ta = Thermal Load for Abnormal Condition

No other loading conditions are considered for this analysis.

Let U be the section moment or shear capacity. The load combination used to establish the structural adequacy of the pool is:

$$U \geq D + Ta$$

## 5.0 INPUT INFORMATION

1. The structural details of the pool structure are taken from the drawings listed in Reference 1.
2. Material Properties:

Reinforcing steel: The type of reinforcing bars used is Grade 40.

Modulus of Elasticity = 29,000,000 psi. (Ref. 2, Section 8.5.2)

Yield strength at 150°F = 39000 psi (Ref. 3)

Concrete:

Compressive strength (Ref. 4),  $f'_c = 3000$  psi

Density of concrete = 150 lb/ft<sup>3</sup>

Modulus of Elasticity,  $E_c$ , is

$$E_c = 57000\sqrt{3000} = 3,122,000 \text{ psi (Ref. 2, Section 8.5.1)}$$

Poisson's ratio = 0.17\*

Coefficient of thermal expansion,  $\alpha_c$ , is

$$\alpha_c = 0.0000055 \text{ in/in/}^\circ\text{F (Ref. 2, Appendix A, Section A.3.3.(d))}$$

\*Poisson's ratio for concrete varies between 0.15 and 0.2. An exact value for any particular concrete type is not known. Consequently, an average value of 0.17 is used.

## 6.0 MATHEMATICAL MODELING

### 6.1 Finite Element Model

The structural analysis of the reinforced concrete spent fuel pool under dead weight and thermal loading is performed using the finite element method and the ANSYS computer code. The walls and the floor of the spent fuel pool are modeled using plate elements having both in-plane and bending displacement capabilities. The rectangular shell element, STIF 43, of ANSYS is used for this purpose. The element accepts uniformly varying thickness, and this option is used in modeling the south wall.

In Figure 1, the model in which the walls have been laid flat in the plane of the floor is shown with the element numbering.

The cross-sections, east-west and north-south, of the spent fuel pool are shown in Figures 2 and 3. The plan at the floor level is shown in Figure 4. The arrangement of walls supporting the pool slab is shown in Figure 5. These figures show the relevant dimensions of the walls and the floor and the thicknesses of these concrete slabs that are used in the analysis.

The dimensions of the floor slab used for the analysis is the distance between the faces of the opposite walls. Such an assumption is appropriate for the analysis of rectangular tanks and is used in Reference 5.

As a result of the heating of the concrete by the pool water, the inner surfaces of the pool walls are hotter than their outer surfaces. Similarly, the top surface of the pool floor is hotter than the bottom surface. Restraint to free thermal expansion is offered by the continuity of the pool structure. This results in elastic strain gradients and hence elastic curvatures being developed across the thickness of the floor and the walls. This in turn results in thermal moments being developed across the cross sections of the pool floor and walls. The nature of the thermal moments is such that the outer surfaces of the walls and bottom surface of the floor are in tension while the inner surfaces are in compression. This condition exists at all locations of the walls and the floor, regardless of whether they are near to or away from the joints.

The design of the pool structure is such that the joints between the walls and the floor can be considered rigid to resist negative bending moments. A negative bending moment is defined as that creating compression on the outside faces of the walls and lower surface of the pool floor. The dead loads on the pool floor and the walls develop negative moments at the joints. Therefore the use of rigid joints in the model for dead loads is appropriate.

The thermal bending moments create tension at the outer surfaces of the walls and the bottom surface of the floor. The reinforcements near the outer surfaces of the north, east and south walls are not continuous with the reinforcement near the bottom surface of the pool floor. These thermal bending moments cannot be transferred from the walls to the floor through the joints. Therefore, these joints are treated as pinned for the thermal stress model. The joints between the west wall and the floor and those between adjacent walls are considered as rigid.

In order to establish a pinned connection between the pool floor and the north, east and south walls, the nodes at the connections are defined with separate node numbers for the walls and the floor. All degrees of freedom between the corresponding nodes with the exception of the rotational degree of freedom that reflects the pinned connection are coupled between the sets of two nodes.

## 6.2 Support Conditions

The manner in which the pool structure is supported by the walls beneath the floor slab is shown in Figures 4 and 5. The modeling of these support walls is depicted in Figures 6 and 7. The floor slab is simply supported on these walls along the north, south, and east edges. It is free along the west edge. Under the given loading, bending moments develop in the wall and floor slabs due to the rigid nature of the joints between the walls and floor. Also, the critical section for shear in the floor slab is along the line where the walls and the floor are connected. These are taken into consideration in deciding the support conditions.

Along the east edge, the floor is supported on an 18 inch thick and 30 inch high reinforced concrete stub wall. The lower end of the wall is fixed to the concrete foundation. The horizontal displacement restraint along this edge is provided by the flexural rigidity of the wall in the east-west direction. The arrangement of the reinforcement at the intersection of the support wall and the floor slab is such that the joint can be considered pinned. The wall offers restraint to horizontal displacement of the floor slab in the direction parallel to the plane of the wall. In this case the wall acts as a deep cantilever beam under shear. The horizontal restraints offered by the support wall both transverse to its plane and parallel to its plane are modeled by elastic translational springs. The vertical support is also modeled by the springs whose stiffness is the same as the axial stiffness of the east support wall.

The vertical wall near the west edge of the floor slab is supported at its bottom end on a 12 inch thick floor slab which is relatively flexible out of plane. This wall, therefore, is not treated as a support. There is a 6 inch wide 4 foot deep vertical shear key along the length of the west wall between this wall and the adjacent concrete around the reactor vessel. This concrete is supported by a thick reinforced concrete wall that goes all the way to the foundation. However, there is a 3/4 inch Fesco board vertical expansion joint between the west wall and the adjacent concrete. Therefore, only the vertical support along the shear key is considered. The west edge of the floor slab is considered to be free.

Along the south edge the floor is supported vertically by a 24 inch thick reinforced concrete wall which is supported at the foundation. Vertical restraint is modeled by vertical springs with their spring constants representing the axial stiffness of the wall in the vertical direction. Horizontal restraint is offered by the rigid plate structure. This structure extends all the way from the east edge to a distance of 18'-6". Beyond this distance and all the way to the west edge, the floor slab is supported by a 3'-6" thick reinforced concrete wall. Horizontal restraint to the displacement of the floor slab is provided by the flexural rigidity of the wall in the north-south direction. Vertical restraint is provided by the axial stiffness of the wall in the vertical direction. The horizontal restraint in the direction parallel to the plane of the wall is provided by the wall acting as a shear wall. Also, the connections at the support are treated as pinned connections.

Along the north edge, the floor slab is supported by the 24 inch thick reinforced concrete wall that extends to the foundation. This wall supports the floor and also provides a certain degree of horizontal restraint due to its flexural rigidity for bending in the north-south direction.

The wall also offers a horizontal restraint to the floor displacement in the direction parallel to the plane of the wall. In this case the wall acts as a cantilever shear wall. Here also, a pinned connection between the support wall and the floor slab is considered.

The various horizontal and vertical restraints offered by the support walls to the displacement of the floor slab are modeled by linear translational springs in the ANSYS model. These springs represent the existing restraints to the pool structure displacements and the forces in the springs give the various forces applied to the support walls. These forces are used in the analysis of the support walls. The ANSYS STIF-40 combination element is used for this purpose.

## 7.0 LOAD CONDITIONS

The two load conditions for the pool structure considered in the analysis are as follows:

1. Dead Weight Loads (D): This load is applied to the walls and floor of the pool structure. For the walls the only load is the horizontal hydrostatic pressure due to the water contained in the pool. For the floor this load consists of the weight of water and the weight of fully loaded racks and other equipment stored in the pool.
2. Abnormal Thermal Load (Ta): This is due to a temperature differential developed across the thickness of the spent fuel pool floor and wall slabs. The temperatures for the thermal stress analysis are determined from a thermal analysis. The maximum temperature of the inside concrete surface is taken to be 150°F.

## 7.1 Hydrostatic and Other Dead Loads

The height of the pool walls is 31 ft. above the pool floor. The level of water is normally 2 ft. below the top level of the walls. However, in the finite element model the walls of the pool are 31 ft. high and for convenience, the pressure is applied assuming the depth of water to be 31 ft. The density of water is  $62.4 \text{ lb./ft}^3$ . The pressure on the floor is therefore 13.4 psi. The ANSYS element STIF 43 accepts only uniform pressure on the surface. The linearly varying pressure is converted to a step varying pressure. These uniform pressures are then applied to the corresponding elements.

The weights of the racks and other equipment are taken from References 6 and 7. Their buoyant weight is 246,200 lbs. The total area over which this load acts (that is the total area of the racks and the equipment) is  $56330 \text{ in}^2$ . Assuming that the total load is uniformly distributed over this area, the intensity of pressure is 4.4 psi. This pressure is applied over the entire floor area of  $74880 \text{ in}^2$ . Applying the total load to the pool floor in this manner results in this load being overestimated by a factor of 1.33 since the entire floor area is considered loaded while in reality only 75% is actually loaded. This overestimate of the equipment weight loading by 33 percent is more than sufficient to account for the approximation made in uniformly distributing this load.

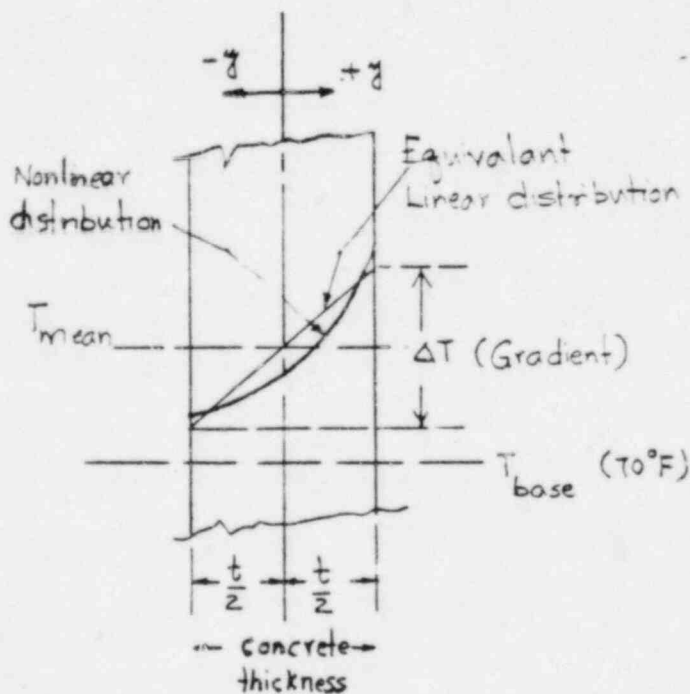
To the water and equipment pressure must be added the additional load due to the weight of the concrete floor slab itself. This additional pressure is 6.2 psi. The total pressure to be applied to the floor is therefore 24 psi.



## 7.2 Thermal Loading

If the pool water should rise in temperature, the pool walls and floor will be heated and will experience a rise in temperature. Thermal gradients will be developed in these structural components eventually resulting in thermal stresses, moments and forces.

The temperature distribution for the specified maximum wall temperature is determined from a thermal analysis. Typical temperature distributions shown in Figure 8 are nonlinear across the thickness of the slab under consideration. For the purpose of the stress analysis these are converted to equivalent linear temperature distributions using the procedure suggested in ACI 349-80. The base temperature of which the concrete is free of thermal stresses is taken as 70°F as suggested in ACI 349-80. The equivalent linear temperature distribution will be a combination of a mean temperature (uniform over the thickness) and a linear gradient (across the thickness). These are expressed as:



$$T_{mean} = \frac{1}{t} \int_{-t/2}^{t/2} T(y) dy - T_{base}$$

$$\Delta T = \frac{12}{t^2} \int_{-t/2}^{t/2} y T(y) dy$$

The integral in the expression for  $\Delta T$  is the moment of the area under  $T(y)$  about the section center line.  $T(y)$  is the nonlinear temperature distribution for this analysis.  $T_{\text{mean}}$  and  $\Delta T$  are determined from the nonlinear temperature distribution by numerical integration using the trapezoidal rule.

The maximum values of  $\Delta T$  from these graphs and the value of  $T_{\text{mean}}$  at this time are used in the analysis.

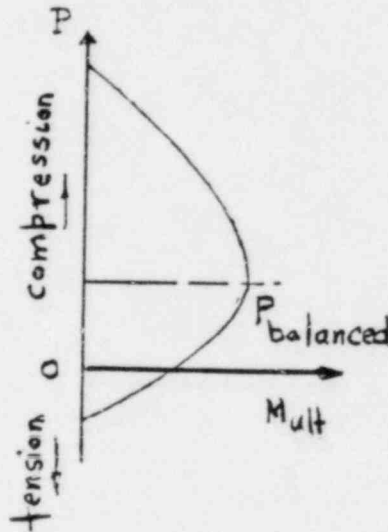
A typical graph of  $T_{\text{mean}}$  and  $\Delta T$  is shown in Figure 9. This thermal loading is applied in seven steps for the abnormal thermal loading case.

## 8.0 SECTION STRENGTH CAPACITIES

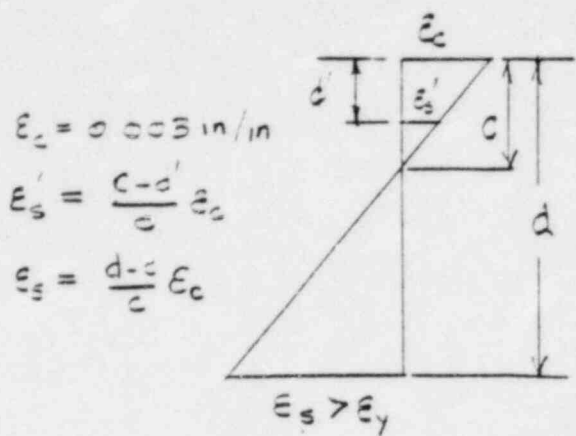
The ANSYS computer runs give the moment and shear at the various locations of the pool structure. The results for the different loads are combined in the manner previously described. These moments and shears are then compared with the section moment and shear capacities to determine the margin of safety.

### 8.1 Moment Capacity

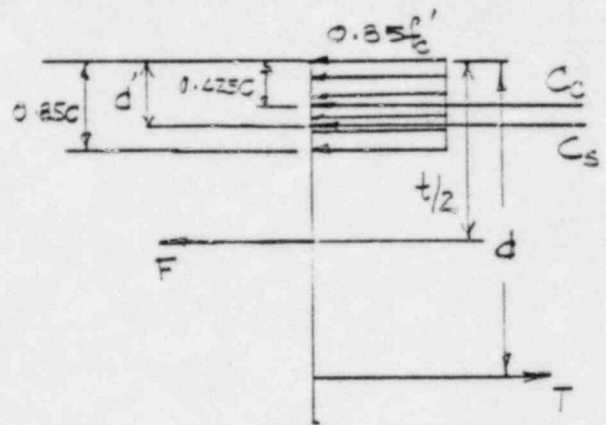
The moment capacities of the sections are calculated using the section properties and are based on the ultimate strength theory (Reference 8). The equations are modified to take into account the axial forces acting on the section. Due to the light reinforcement and large depths of the sections, the steel tension controls the ultimate capacity and the calculations fall in the region below the  $P_{balanced}$  line in the interaction diagram shown below.



The existence of axial force influences the moment and shear capacities. In general tensile axial force decreases the section strength capacities whereas compressive axial force increases the strength capacities. For beam shear or one-way action the effect of axial forces on shear capacity is determined according to ACI 349-80 Section 11.3.1.2 (Eq. 11-4) for compressive axial force and Section 11.3.2.3 (Eq. 11-9) for tensile axial force. For local shear or two-way action the effect of axial forces on shear capacity is determined according to ACI 349-80 Section 11.11.2.2 (Eq. 11-37a, 11-37b and 11-37c). The axial forces that occur in the pool structure are considered in calculating the section moment capacity in the following manner.



Strain Diagram



Force Diagram

Note: F is the external force on the section;  $C_c$ ,  $C_s$ , and T are the internal forces.

The strain and force diagrams are shown in the sketches above. Consider a 1 foot width of the slab. Using force equilibrium and strain compatibility, the neutral axis depth C is calculated from:

$$(12)(0.85f_c')(0.85)c + 87000A_s'\left(\frac{c-d'}{c}\right) - A_s f_y + F = 0$$

F is treated positive if in tension. The stress in compression steel is calculated as

$$f_s' = (87000)\left(\frac{c-d'}{c}\right)$$

If  $|f_s'| > |f_y|$ , C is recalculated using  $f_s' = f_y$

Once the depth of the neutral axis from the compression edge is determined, the ultimate moment capacity is calculated from

$$\begin{aligned}
 M_{ult} = & (0.9) \left[ (8.67f_c')(c)(d - 0.425c) \right. \\
 & \left. + A_s' f_s' (d - d') + F \left( d - \frac{t}{2} \right) \right] / 12 \frac{\text{in-lb}}{\text{in}}
 \end{aligned}$$

## 8.2 Shear Capacity

Since no shear reinforcements are provided, the average shear strength capacities of concrete for a section extending in a plane across the entire width are calculated from

$$\phi V_c = 2 \phi \sqrt{f'_c} b d \left( 1 + \frac{F}{2000 A_g} \right) \quad \text{Ref. 2, Eq. 11-4}$$

when the axial force  $F$  is positive in compression, and

$$\phi V_c = 2 \phi \sqrt{f'_c} b d \left( 1 + \frac{F}{500 A_g} \right) \quad \text{Ref. 2, Eq. 11-9}$$

when  $F$  is negative in tension.  $\phi$  is equal to 0.85.  $b$  and  $d$  are defined on page 9-3.

The local shear strength capacities checked on an element by element basis are calculated from

$$\phi V_c = \phi (V_{c1} + V_{c2}) \quad \text{Ref. 2, Eq. 11-37a}$$

where

$$V_{c1} = 4 \sqrt{f'_c} b_1 h \sqrt{1 + \frac{f_{m1}}{4 \sqrt{f'_c}}} \quad \text{Ref. 2, Eq. 11-37b}$$

$$V_{c2} = 4 \sqrt{f'_c} b_2 h \sqrt{1 + \frac{f_{m2}}{4 \sqrt{f'_c}}} \quad \text{Ref. 2, Eq. 11-37c}$$

where  $f_{m1}$  ( $f_{m2}$ ) is the membrane stress in the slab or wall acting over  $b_1$  ( $b_2$ ), to be taken as positive for compression and negative for tension.  $\phi$  is equal to 0.85.  $h$  is the slab thickness.  $b_1$  and  $b_2$  are the total lengths of that portion of the perimeter for which  $V_{c1}$  and  $V_{c2}$  are computed.

### 8.3 Required Development Length

Required development and lap splice lengths were calculated in accordance with ACI 349-80, Chapter 12. Per this code, the basic development length of rebars in tension is given as follows:

$$\text{Basic } l_d = 0.04 A_b f_y / \sqrt{f'_c}$$

But not less than  $.0004 d_b f_y$ .

Additional applicable factors shall be

1. 0.8 for bars laterally spaced 6" apart minimum.
2. 1.4 for top reinforcement, which is horizontal reinforcement so placed that more than 12 inches of concrete is cast in members below the reinforcement.
3.  $(A_s \text{ required} / A_s \text{ provided})$ , when reinforcement in a flexural member is in excess of that required by analysis.

In no case shall  $l_d$  be less than 12 inches.

The tension lap splices can be divided into three classes per ACI 349-80, Section 12.16.2

**TABLE 12.16 – TENSION LAP SPLICES**

$\frac{A_s \text{ provided}^*}{A_s \text{ required}}$	Maximum percent of $A_s$ spliced within required lap length		
	50	75	100
Equal to or greater than 2	Class A	Class A	Class B
Less than 2	Class B	Class C	Class C

\*Ratio of area of reinforcement provided to area of reinforcement required by analysis at splice location

Minimum length of lap for tension lap splices shall be as required for Class A, B, or C splice, but not less than 12 in., where:

- Class A splice . . . . .  $1.0 l_d$   
 Class B splice . . . . .  $1.3 l_d$   
 Class C splice . . . . .  $1.7 l_d$

In one location, namely in the south wall at 5'-6" from the east wall (see Figure 4), the lap splice was not sufficient to meet the ACI 349-80 criteria. For this case, a calculation was performed which took into account the particular grade reinforcement and amount of cover provided in the design. This was done as follows. From Ref. 9, which is referred to in the Commentary on ACI 318-77 as reference 12.3, it was proposed, after a nonlinear regression analysis of test results of beams with lap splices taking into account the effects of length, cover, clear spacing between splices, bar diameter, concrete strength, and transverse reinforcement, that "the length of a tension lap splice  $l_s$  shall be computed as for development length  $l_d$  with appropriate cover  $C$  determined from a consideration of the clear cover and the clear spacing between the splices", and "for deformed bars in tension the development length  $l_d$  (in inches) shall be computed as the product of (a) the basic development length and (b) the applicable modification factors."

The basic development length for Grade 60 reinforcement is

$$l_d = \frac{10200 d_b}{\sqrt{f'_c} \left( 1 + 2.5 \frac{c}{d_b} + K_{tr} \right) \phi}$$

where  $d_b$  = Diameter of rebar  
 $\phi$  = 0.8 = Capacity reduction factor  
 $K_{tr}$  = Coefficient to account for transverse reinforcement  
 $C$  = lesser of clear cover or clear spacing between splices

Per Ref. 9, in our case, the applicable modification factors (i.e., the factors by which the above expression is to be multiplied) are 0.6 for Grade 40 reinforcement and 1.3 for top reinforcement.

## 9.0 ANALYSIS METHOD

### 9.1 Thermal Stress Analysis

When the thermal gradients are applied to the initially uncracked cross section of the pool walls, the restraints to rotation will cause moments to be developed in these sections. The magnitude of these thermal moments is a function of the degree of the restraint, stiffness of the cross section, and the applied thermal gradient.

For a given restraint and thermal gradient, the thermal moment is a linear function of the flexural rigidity of the cross section. The thermal moment increases with the thermal gradient until the extreme fiber tensile stress in the cross section reaches the value of the modulus of rupture of the concrete. As soon as the extreme fiber stress exceeds the modulus of rupture, the tension concrete cracks thereby reducing the section stiffness considerably. This relieves and reduces the thermal moment considerably. In a continuous structure with varying degrees of restraint and stiffness, the process of cracking, changing of the structure stiffness, thermal moment relief and redistribution takes place continuously with the increase in the thermal gradient until the maximum applied thermal gradient is reached. The thermal moment at any stage of the heating is dependent on the continuous changes in the stiffness caused by the thermal gradient up to and including that stage. The problem is nonlinear in nature. In this analysis it is solved using a step-by-step procedure by applying the  $T_{\text{mean}}$  and  $\Delta T$  sequentially.

In the present case  $T_{\text{mean}}$  and  $\Delta T$  are applied in seven steps. Since the temperature at the two surfaces of the slabs are to be input into ANSYS,  $T_{\text{in}}$  (inside temperature) and  $T_{\text{out}}$  (outside temperature) at each step are calculated from  $T_{\text{mean}}$  and  $\Delta T$ . For the first step  $0.4T_{\text{mean}}$  and  $0.4\Delta T$  are applied and a thermal stress analysis is performed. These values are chosen on the consideration that the cracking is initiated in the structure at approximately this temperature level. The cracked status of the structure is determined on an element-by-element basis by comparing the sum of the deadweight and the thermal extreme fiber tensile stress (just calculated) in each direction, that is X and Y, with the modulus of rupture  $f_r$ . The modulus of rupture  $f_r$



is equal to  $7.5\sqrt{f'_c}$ . If an element is found cracked in any of its two orthogonal directions (parallel to the reinforcements) the moment of inertia in that direction is changed from  $I_g$  to  $I_{cr}$ . In calculating  $I_{cr}$ , consideration is given to the sign of the total bending moment. Positive bending moments create tension at the outer surfaces of the wall and bottom surface of the floor. With these changes in the finite element model implemented, the thermal input corresponding to  $0.5 T_{mean}$  and  $0.5 \Delta T$  is applied and a thermal analysis performed. The model is updated based on the total extreme fiber tensile stresses at this stage and the next step temperature applied. This procedure is carried on step-by-step till the specified  $\Delta T$  and the associated  $T_{mean}$  are reached. At the temperatures where the forces and moments are to be calculated for the load combinations, several calculational iterations are required. This accounts for the effects of cracking up to and including this temperature. The status after two iterations was found to be acceptably stable. Two iterations were performed for  $0.6 \Delta T$  and  $0.8 \Delta T$  cases. For maximum  $\Delta T$  and associated  $T_{mean}$  an additional iteration was performed. Therefore, three iterations were performed for this case.

The shear forces develop primarily as a result of gradients in the thermal bending moments. The magnitudes of these forces depend on the values of the bending moments and the manner in which they change along any section. These bending moments are a function of the thermal gradient and structure stiffness, the latter depending upon the nature of cracking of the structure. Therefore, shear forces are calculated at several stages of heating, such as for  $0.6 \Delta T$ ,  $0.8 \Delta T$  and  $\Delta T$ , and compared to the shear capacities. Since the bending moments are relieved and redistributed to neighboring regions of the cracked section, they are compared to the moment capacities after application of the maximum thermal gradient.

ANSYS plate element stiffnesses are calculated from the plate thickness and  $\Gamma$ . It is not possible to input different thicknesses in the two directions of cracking. Also, the thermal curvature is calculated using the overall thickness of the plate. Therefore, the orthotropic nature of the elements is introduced by using different values of the elastic moduli  $E_x$  and  $E_y$ .

First the moment of inertia of the cracked section is calculated in the two directions. In the uncracked region,  $E_x$  (or  $E_y$ ) is given the value  $E_c$ . In the cracked region the

value of  $E_x$  (or  $E_y$ ) used is  $E_{cr} = E_c I_{cr} / I_g$ . This is done on an element by element basis and a new finite element model is developed. The calculation of the moment of inertia of the cracked sections is described below.

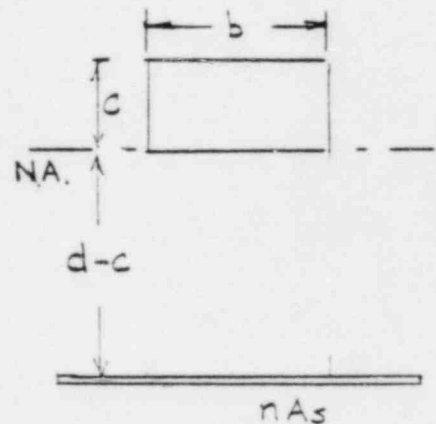
- $E_s$  = modulus of elasticity of steel reinforcement
- $E_c$  = modulus of elasticity of the concrete
- $n = E_s / E_c$
- $c$  = distance of the neutral axis from the compression face.
- $b, d$  = width and effective depth of the section.
- $A_s$  = Area of tension reinforcement
- $A = bc + nA_s$
- $I_g$  = uncracked section moment of inertia.
- $I_{cr}$  = cracked section moment of inertia.
- $f_r$  = modulus of rupture of the concrete.

Taking moment about the compression face,

$$(A)(c) = \frac{bc^2}{2} + nA_s d$$

or  $\frac{bc^2}{2} + nA_s c - nA_s d = 0$

$$c = \frac{-nA_s \pm \sqrt{n^2 A_s^2 + 2nA_s b d}}{b}$$



and  $I_{cr} = \frac{bc^3}{3} + nA_s (d-c)^2$  in.<sup>4</sup>/ft for  $b = 12$  in

or  $I_{cr} = \frac{1}{12} \left[ \frac{bc^3}{3} + nA_s (d-c)^2 \right]$  in.<sup>4</sup>/in. ( $b = 12$  in.)

In these calculations the compression steel is not considered.

The values of  $f_r$ , of the concrete and the uncracked section moment of inertia,  $I_g$  are given by

$$f_r = 7.5 \sqrt{f'_c}$$

$$I_g = \frac{bt^3}{12}$$

where  $t$  = overall depth of concrete.

## 9.2 Support Wall Analysis

In the ANSYS finite element model the support walls are represented by springs, the spring constants of which are so determined as to provide the degree of restraint offered by the support walls to pool floor displacements. Since these springs are provided only at the nodes along the edges of the pool floor, each of them provides the integrated effect of the strip of the wall it represents. For instance, in Figure 10 the spring element (1) represents the shaded strip 'abcd' of the wall, spring element (3) represents the shaded strip 'efgh' of the wall and so on. The forces on the wall act along the top edge 'aq'. The output from the ANSYS computer analysis consists of forces in the springs, and they represent the total force applied over the length of the elemental strips of the wall. These forces are converted to a uniformly distributed load on the walls and then used to determine the structural adequacy of the walls.

These forces on the walls consist of axial, transverse (or out-of-plane) shear and in-plane shear forces. The support walls are checked for the transverse shear force, the bending moment at the base of the wall due to this transverse shear force and the in-plane shear force. The effect of axial forces are considered with the bending moment and the shear forces while determining the section strength capacities. Wherever appropriate, the effect of slenderness ratio and moment magnification factor are considered while analyzing the walls. Especially, ACI 349-80 Sections 10.11.3, 10.11.4, 10.11.5, 11.10.6 and 11.10.7 are used in determining the structural adequacy of the walls.

## 10.0 REFERENCES

1. Big Rock Point; Bechtel Drawings, Job No. 3159
  - a) A-101, Rev. 3, Reactor Building Plan El. 573'0", 585'6" and 611'3".
  - b) A-102, Rev. 2, Reactor Building Plan El. 616'0", 621'0", and 632'6".
  - c) C-113, Rev. 7, Reactor Building Plan El. 599'6".
  - d) C-111, Rev. 8, Reactor Building Plan El. 585'6".
  - e) C-114, Rev. 8, Reactor Building Sections and Plans.
  - f) C-115, Rev. 7, Reactor Building Plan El. 632'6".
  - g) C-117, Rev. 10, Reactor Building East-West Section.
  - h) C-118, Rev.6, Reactor Building East-West Section of Face of Steam Drain Enclosure.
  - i) C-119, Rev. 5, Reactor Building Sections and Details.
  - j) C-121, Rev. 5, Reactor Building North-South Section through Spent Fuel Storage.
  - k) C-107, Rev. 6, Reactor Building Plan of Floor at Elevation 573'0".
2. ACI Standard 349-80, Code Requirements for Nuclear Safety Related Concrete Structures, 1980.
3. ASME Boiler and Pressure Vessel Code; Section III, Division 1, Appendices, 1977 Edition, pages 36-37.
4. "Reports on Concrete Compression Test", Walter H. Flood & Co., dated July 17 & 20, August 7, 10, & 18, September 1, & 13, and October 9, 1961.
5. "Rectangular Concrete Tanks", Portland Cement Association, ST63, 1951.
6. Letter JENK 117-82 dated July 21, 1982 from R. Jenkins of CPCo to H. Eckert of NUS.
7. NUS Report 3312, Rev. 1, "Structural Analysis of the Spent Fuel Racks for Big Rock Point Plant, April 24, 1979.
8. R. Park and T. Paulay, Reinforced Concrete Structures, John Wiley and Sons, 1975.
9. Orangun, C.O., Jirsa, J.O., and Breen, J.E., "A Re-evaluation of Test Data on Development Length and Splices," ACI Journal, Proceedings V.74, Mar. 1977, pp. 114-122.





\* ACTUAL DEPTH OF THE EAST WALL IS 7'-6" FOR CONVENIENCE IN MODELING, A CONSERVATIVE VALUE OF 8'-6" IS USED.

Figure 2 - East-West Section through the Spent Fuel Pool

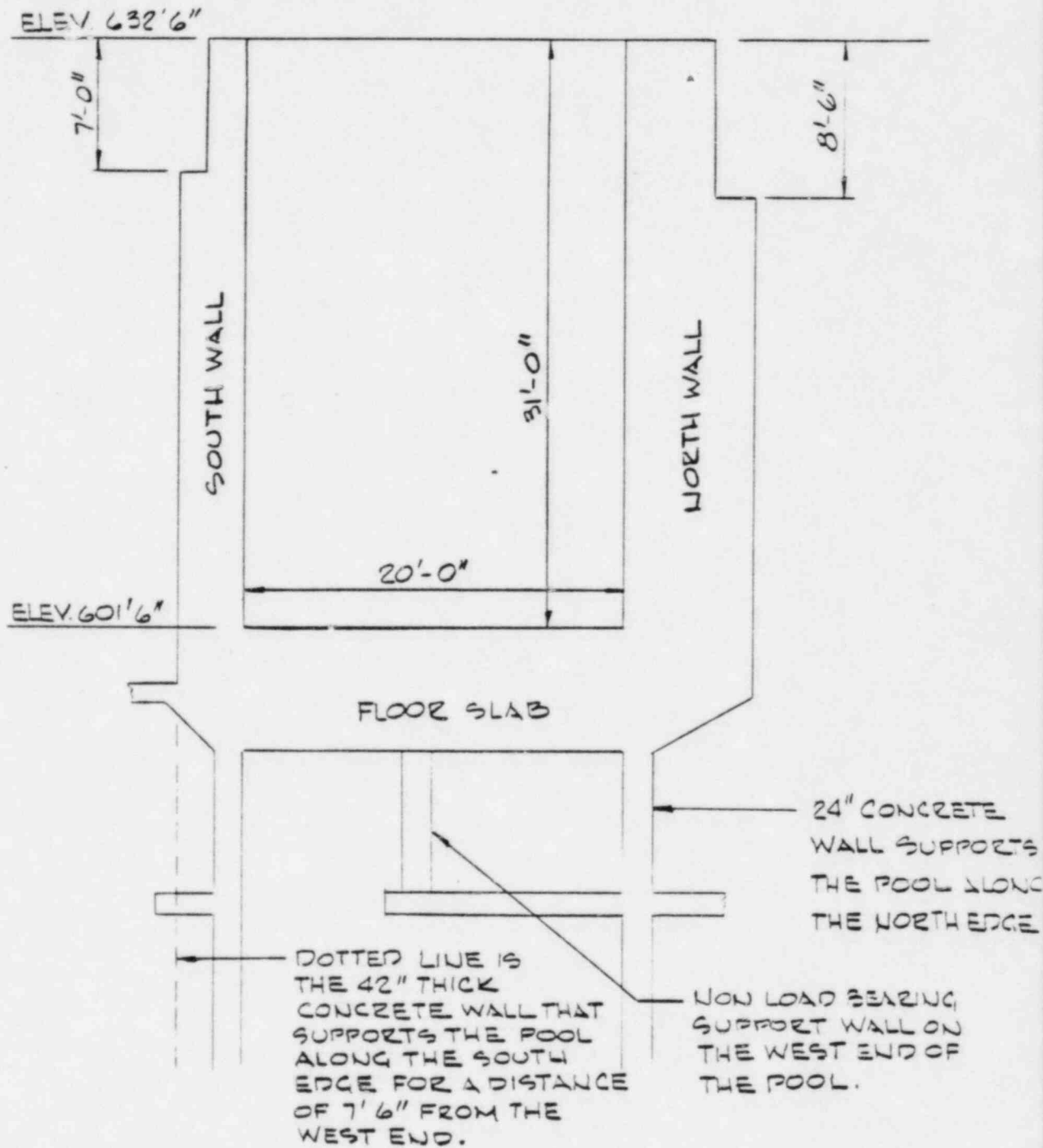


Figure 3 - North-South Section through the Spent Fuel Pool



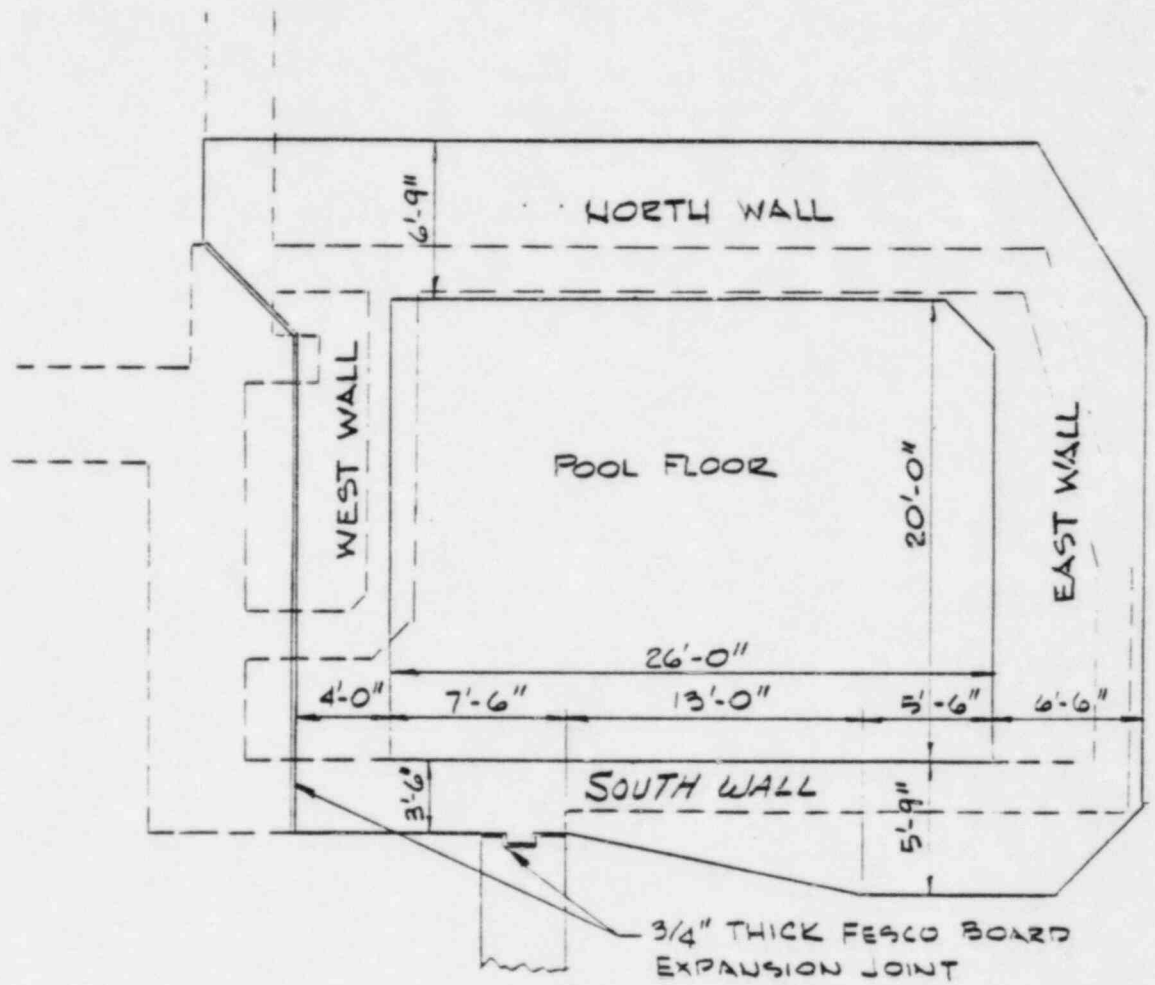


Figure 4 - Plan at the Pool Floor Elevation

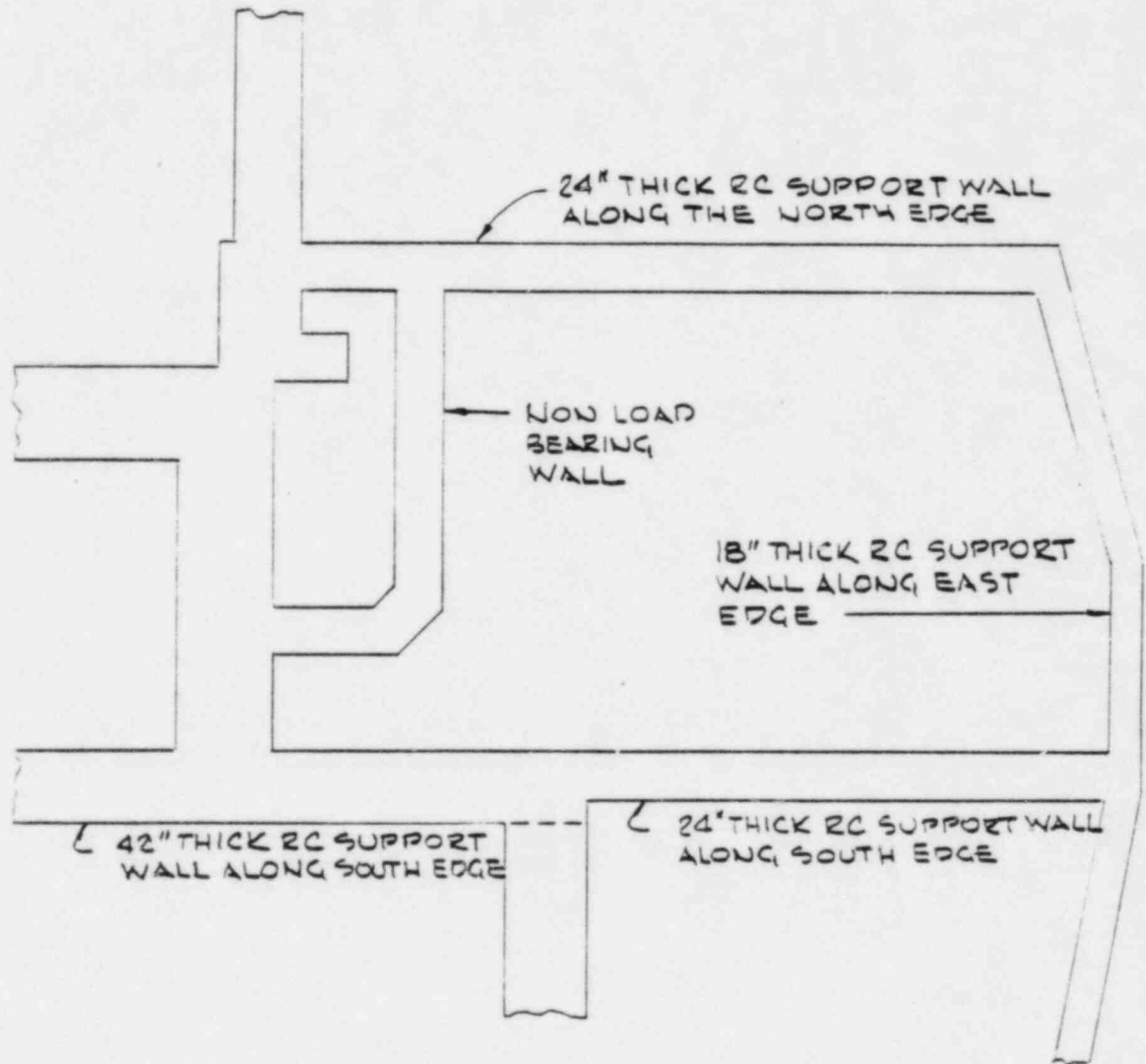


Figure 5 - Plan Section below Elevation 598'0"

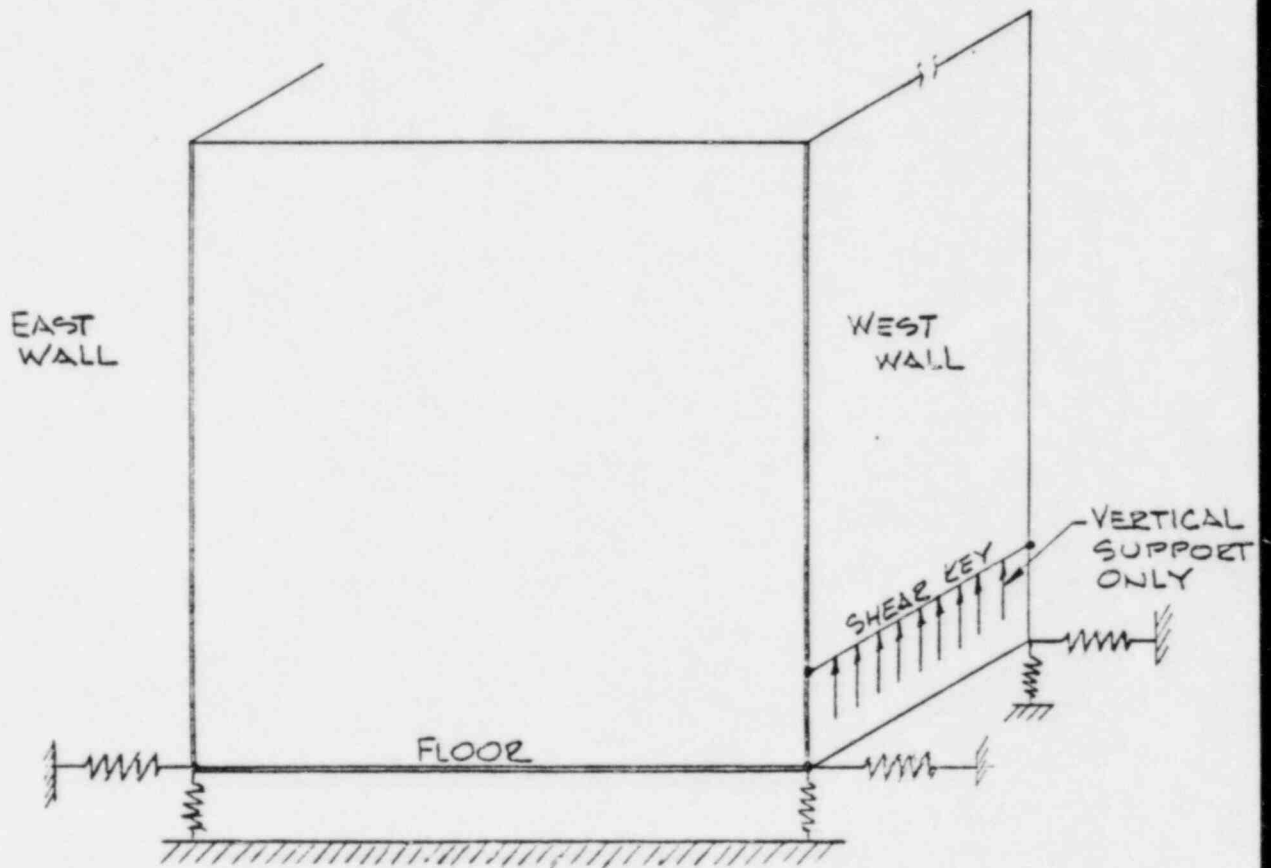


Figure 6 - Floor Support along the East and West Edges

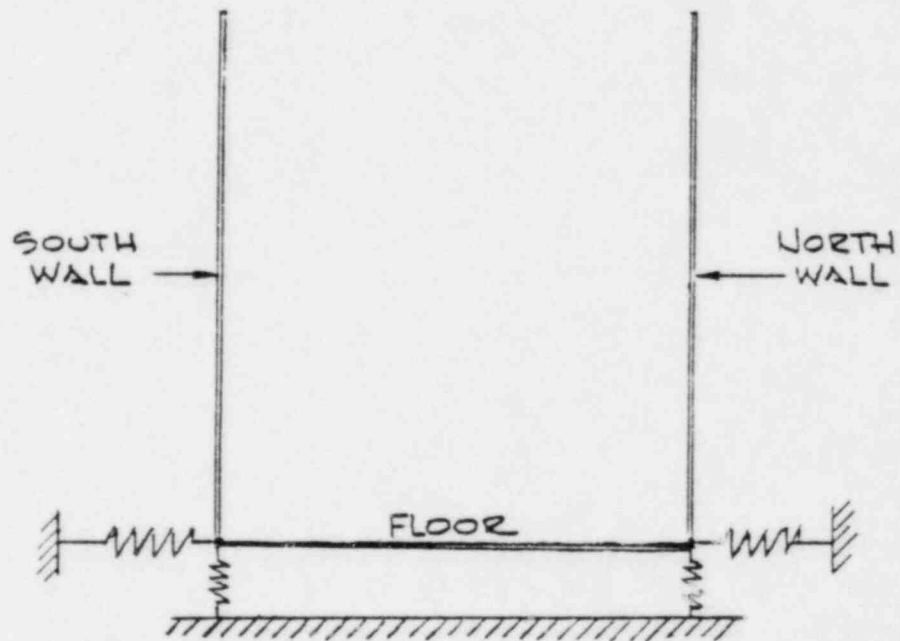


Figure 7 - Floor Support along the North and South Edges

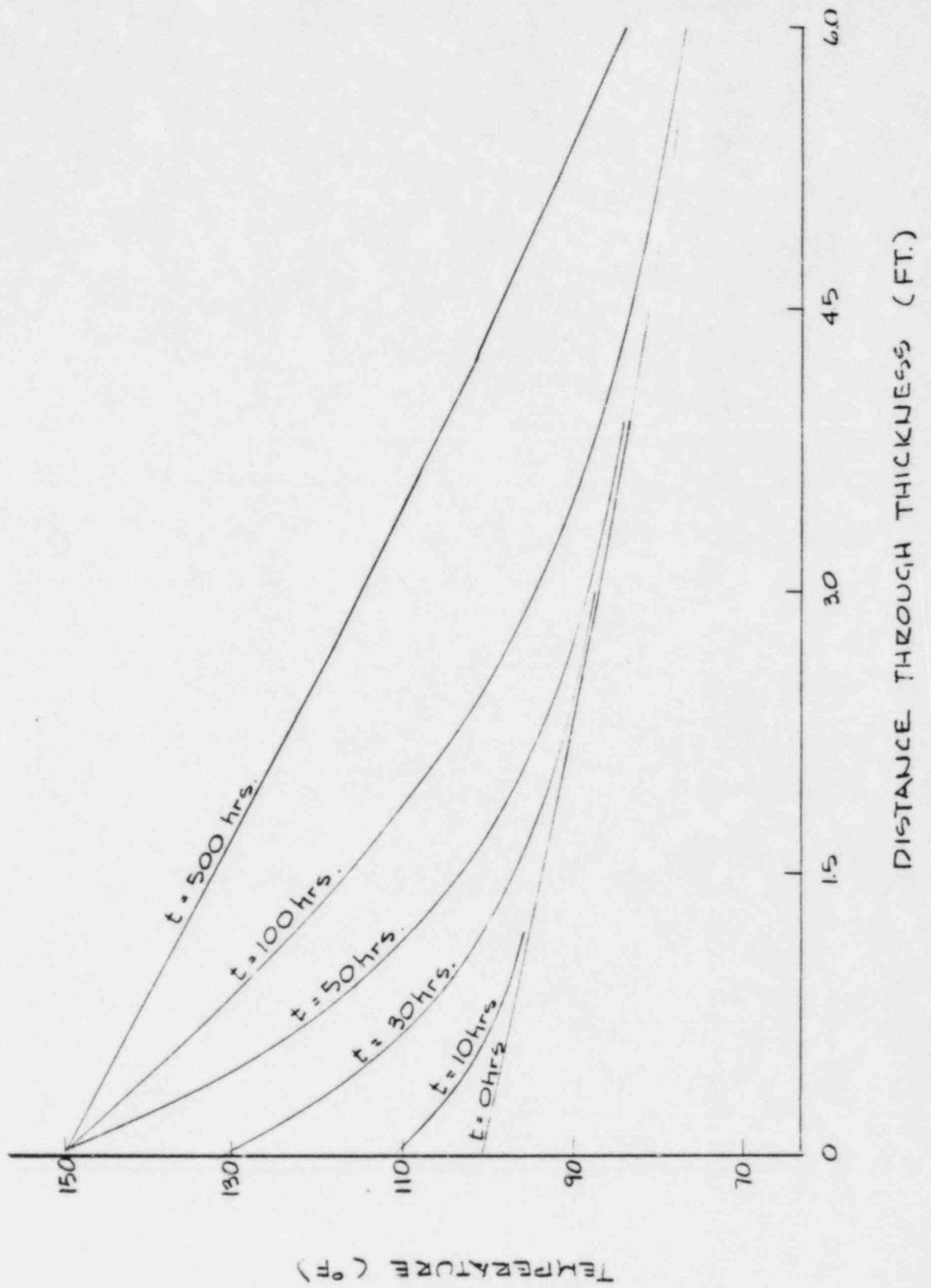


Figure 8 - Typical Temperature Gradients

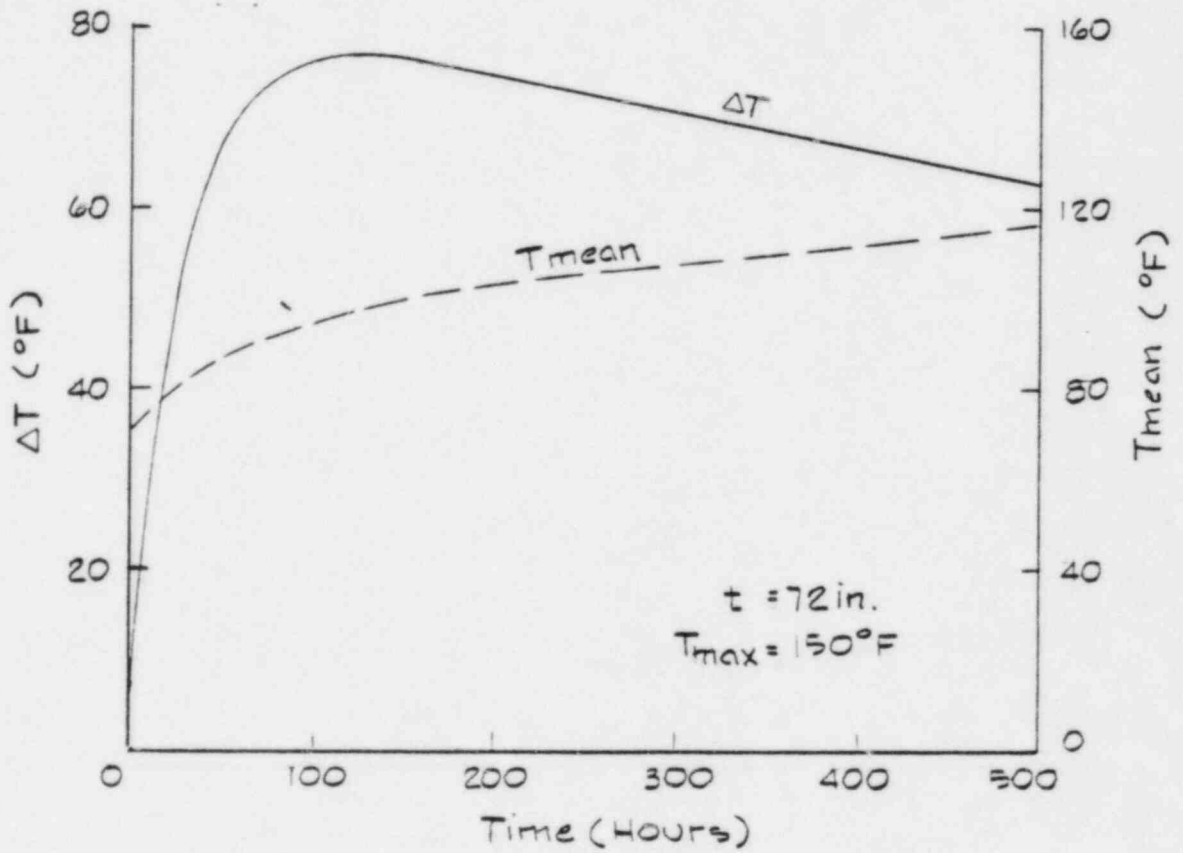


Figure 9 - Typical Variation of  $T_{mean}$  and  $\Delta T$  with Time

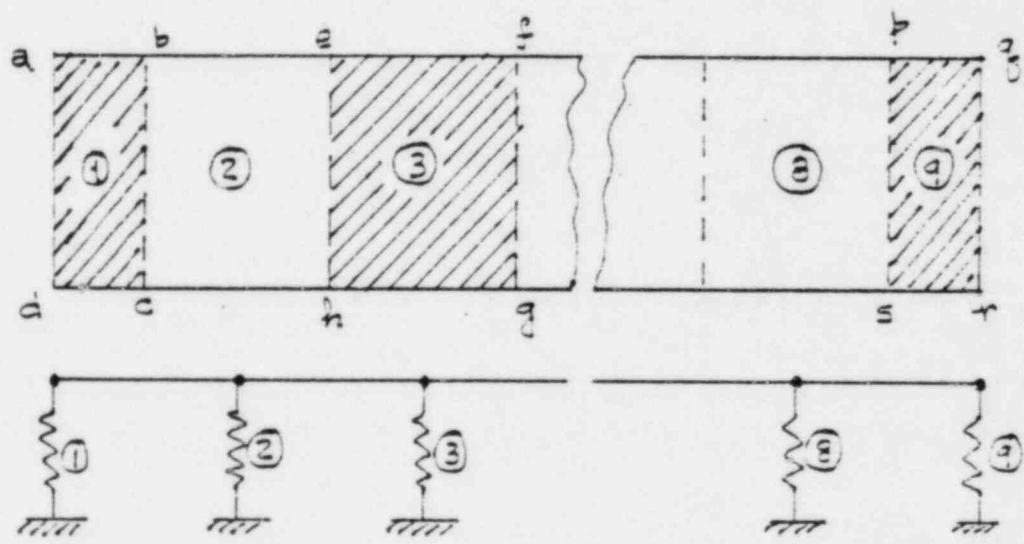


Figure 10 - Typical Support Wall Model

APPENDIX II

Part B

SPENT FUEL POOL  
THERMAL-HYDRAULIC ANALYSIS

Amendment 2 - Dated January 1983

to

Big Rock Point Plant

Spent Fuel Rack Addition  
Consolidated Environmental  
Impact Evaluation,  
Description and Safety Analysis

Consumers Power Company